Turkish Journal of Electrical Engineering & Computer Sciences

http://journals.tubitak.gov.tr/elektrik/

Research Article

Turk J Elec Eng & Comp Sci
(2016) 24: 1901 – 1915

doi:10.3906/elk-1312-131

Classification of short-circuit faults in high-voltage energy transmission line using energy of instantaneous active power components-based common vector approach

Mehmet YUMURTACI[1,*], Gökhan GÖKMEN[2], Çağrı KOCAMAN[3], Semih ERGİN[4], Osman KILIÇ[5]

[1]Department of Electrical Education, Faculty of Technical Education, Afyon Kocatepe University, Afyonkarahisar, Turkey

[2]Department of Mechatronic Engineering, Faculty of Technology, Marmara University, İstanbul, Turkey

[3]Department of Airframe and Powerplant Maintenance, School of Civil Aviation, Ondokuz Mayıs University, Samsun, Turkey

[4]Department of Electrical and Electronics Engineering, Faculty of Engineering, Eskişehir Osmangazi University, Eskişehir, Turkey

[5]Department of Electrical and Electronics Engineering, Faculty of Engineering, Marmara University, İstanbul, Turkey

Received: 18.12.2013 • **Accepted/Published Online:** 01.07.2014 • **Final Version:** 23.03.2016

Abstract: The majority of power system faults occur in transmission lines. The classification of these faults in power systems is an important issue. In this paper, the real parameters of a 28 km, 154 kV transmission line between Simav and Demirci in Turkey's electricity transmission network is simulated in MATLAB/Simulink. Wavelet packet transform (WPT) is applied to instantaneous voltage signals. Instantaneous active power components are obtained by multiplying instantaneous currents obtained from a voltage source side with these WPT-based voltage signal components. A new feature vector extraction scheme is employed by calculating the energies of instantaneous active power components. Constructed feature vectors are treated with a classifier for short-circuit faults that occurred in high-voltage energy transmission lines; this is known as the common vector approach (CVA). This is the first implementation of CVA in the classification of short-circuit faults that occurred in high-voltage energy transmission lines. Furthermore, the same feature vector is applied to a support vector machine and artificial neural network for a comparison with the CVA method regarding classification performance and testing duration issues. Additionally, a graphical user interface is designed in MATLAB/GUI. Various noise levels, source frequencies, fault distances, fault inception angles, and fault exposure durations can be investigated with this interface. Classification of short-circuit faults in high-voltage transmission line is achieved by using an offline monitoring methodology. It is concluded that a combination of the proposed feature extraction scheme with the CVA classifier gives substantially high performance for the classification of short circuit faults in transmission line.

Key words: Common vector approach, support vector machine, artificial neural network, wavelet packet transform, fault classification, short circuit, transmission line

1. Introduction

Faults occurring in transmission lines constitute 85%–87% of overall power system faults [1]. Symmetric and asymmetric short circuits happen when transmission line conductors contact each other or the ground as a result of various physical effects [2]. A rapid and accurate determination of fault type is necessary so that the faulty zone in the electrical line is deactivated immediately to reduce the adverse impacts resulting from substantially high magnitudes of short-circuit circumstances.

*Correspondence: mehmetyumurtaci@aku.edu.tr

Fourier transform (FT), short-time Fourier transform (STFT), and wavelet transform (WT) are the most widely used signal processing methods in determining fault characteristics. FT is applied to obtain only frequency components of stationary signals, but time information is lost. STFT is used for time information requirements in processing nonstationary signals. However, missing data occur in transient analysis of STFT, since it examines signals by dividing equal time intervals. WT is widely preferred in fault classifications, because it treats signals in both frequency and time domains. In WT, the low-frequency components of the signal are analyzed by using large time intervals, whereas the high-frequency components are treated by using small time intervals.

Only current/voltage data or the combination of current and voltage data are exploited in transmission line fault classification studies. In the literature, measured voltage data can be input, and discrete wavelet transform (DWT) is applied to this input signal [3,4]. The components calculated from DWT are classified with using artificial neural network (ANN) classifier [3]. Energies of voltage signals were also utilized in [4]. When measured current signal is used, DWT decomposition draws attention. For transmission line fault detection, Chanda et al. [5] investigated the absolute value of the current peaks, the average value of the current signals, and three-level DWT detail coefficients, while Geethanjali and Priya [1] employed five-level DWT components of current signals and used an ANN as a classifier. DWT and fuzzy logic were combined as an alternative study [6]. Entropy values of DWT components obtained from current data were preferred in the study of El Safty and El-Zonkoly [7]. Upendar et al. [8] used nine-level DWT coefficients and a perceptron neural network as classifiers, whereas Abdollahi and Seyedtabaii [9] employed an ANN with three-level approximation and detail coefficients. In addition, Samantaray [10] applied S-transform to current signals and obtained a feature vector with energy, standard deviation, variance, and autocorrelation components calculated from these signals. The systematic fuzzy rule-based approach was used [10].

In addition to the above-mentioned studies, several experiments based on both current and voltage data were implemented for transmission line fault diagnosis. Joorabian et al. [11] developed a fault classifier that uses discrete Fourier transform (DFT) of both current and voltage signals with radial basis function networks. Jamehbozorg and Shahrtash [12] applied one-phase voltage and odd harmonics of the remaining two phases to a decision tree classifier. He et al. [13] developed a new classification scheme that uses WT, singular value decomposition, and Shannon entropy. Ekici [14] preferred the entropy of DWT components, while Çöteli [15] classified transmission line faults by incorporating the S-transform with an SVM classifier.

In this paper, first, WPT is applied to three-phase voltage values. Second, the components of instantaneous active power are calculated by multiplying current values with WPT-based voltage components for each phase. Third, a feature extraction process is carried out by obtaining the energies of these components. This feature vector is then applied to CVA, SVM, and ANN. These classifiers are compared with respect to their recognition accuracies, training, and testing times. Furthermore, white Gaussian noise (WGN) that is between 20 and 50 dB SNR value is added to the signals, and the effects of noise are examined. Finally, MATLAB/GUI is used for a visual demonstration of fault cases and a fault type classification using different classifiers.

2. Wavelet packet transform

A wavelet is a form of wave limited in time whose average value is zero [16]. WT has the ability to analyze various power quality problems. The application areas of wavelets include electromagnetic wave analysis, filters, time and frequency analysis of different patterns, image processing, transient analysis of electrical signals, and data compression techniques [17]. Wavelets have various window sizes. They are wide for slow frequencies and

narrow for fast frequencies [18]. WT can be carried out in two ways, namely continuous wavelet transform (CWT) and DWT. DWT is preferred because it is faster than CWT [19].

The most important factor in WT is to determine the level of decomposition and the mother wavelet. The decomposition level is adjusted by the sampling frequency of the original signal [20]. When WT is applied to a signal, several components having different frequency values of the signal can be found by doing scaling and shifting with the mother wavelet. The high-scale, low-frequency components of the signal produced by low-pass filtering are called approximations, and these are indicated as 'A' in Figure 1. The low-scale, high-frequency components of the signal produced by a high-pass filter are known as details, and these are indicated as 'D' in Figure 1 [21].

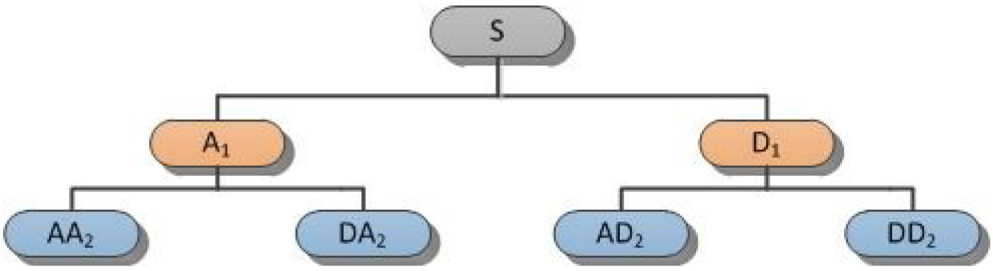

Figure 1. Decomposition of a two-level WPT of the S signal.

WPT gives more information than DWT. A two-level WPT of the S signal is illustrated in Figure 1. The subscripts in this figure indicate the level of the WPT.

In this paper, the sampling frequency is selected as 3.2 kHz. Four-level WPT is applied to obtain the bandwidth that is closest to the fundamental frequency of 50 Hz. db20, which belongs to the Daubechies wavelet family, is preferred as the mother wavelet [22,23]. The frequency bandwidths of 16 components obtained for each phase are given in Table 1.

Table 1. Frequency bandwidths of components obtained by using four-level WPT of a signal sampled at 3.2 kHz.

WPT component	Frequency bandwidth (Hz)	WPT component	Frequency bandwidth (Hz)
$AAAA_4$	0–100	$AAAD_4$	800–900
$DAAA_4$	100–200	$DAAD_4$	900–1000
$ADAA_4$	200–300	$ADAD_4$	1000–1100
$DDAA_4$	300–400	$DDAD_4$	1100–1200
$AADA_4$	400–500	$AADD_4$	1200–1300
$DADA_4$	500–600	$DADD_4$	1300–1400
$ADDA_4$	600–700	$ADDD_4$	1400–1500
$DDDA_4$	700–800	$DDDD_4$	1500–1600

3. Power system simulation model

The simulation of the 28 km, 154 kV transmission line between Simav and Demirci is achieved in MATLAB/Simulink using real parameters given in [24]. The corresponding power system model is given in Figure 2. Parameters of equipment used in the model are presented in the Appendix. The ground resistance and fault resistances are fixed as 0.001 Ω. The identification and classification of short-circuit faults occurring in the transmission line are performed under variable conditions such as source frequency, fault inception angle, fault time, and fault distance.

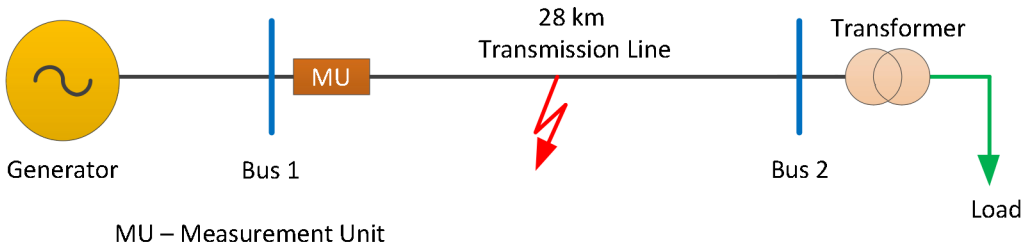

Figure 2. Power system model of the simulated transmission line.

Phase short-circuit types and the corresponding class labels are given in Table 2, along with a number of signals belonging to 10 different short-circuit faults, which are either symmetrical or asymmetrical in the simulation model of the system. Three-phase instantaneous voltage and current waveforms measured at the beginning of the line are shown in Figure 3 for nonfaulty and faulty conditions in ABCG, ABG, AB, and AG phase short-circuit circumstances. Short circuits of these phases occur at 14 km of the transmission line and are investigated in an interval of 0.04–0.1 s. The power system operating frequency is 50 Hz. In any short circuit condition, the voltages of faulty phase(s) decrease, whereas the current passing through them rises significantly.

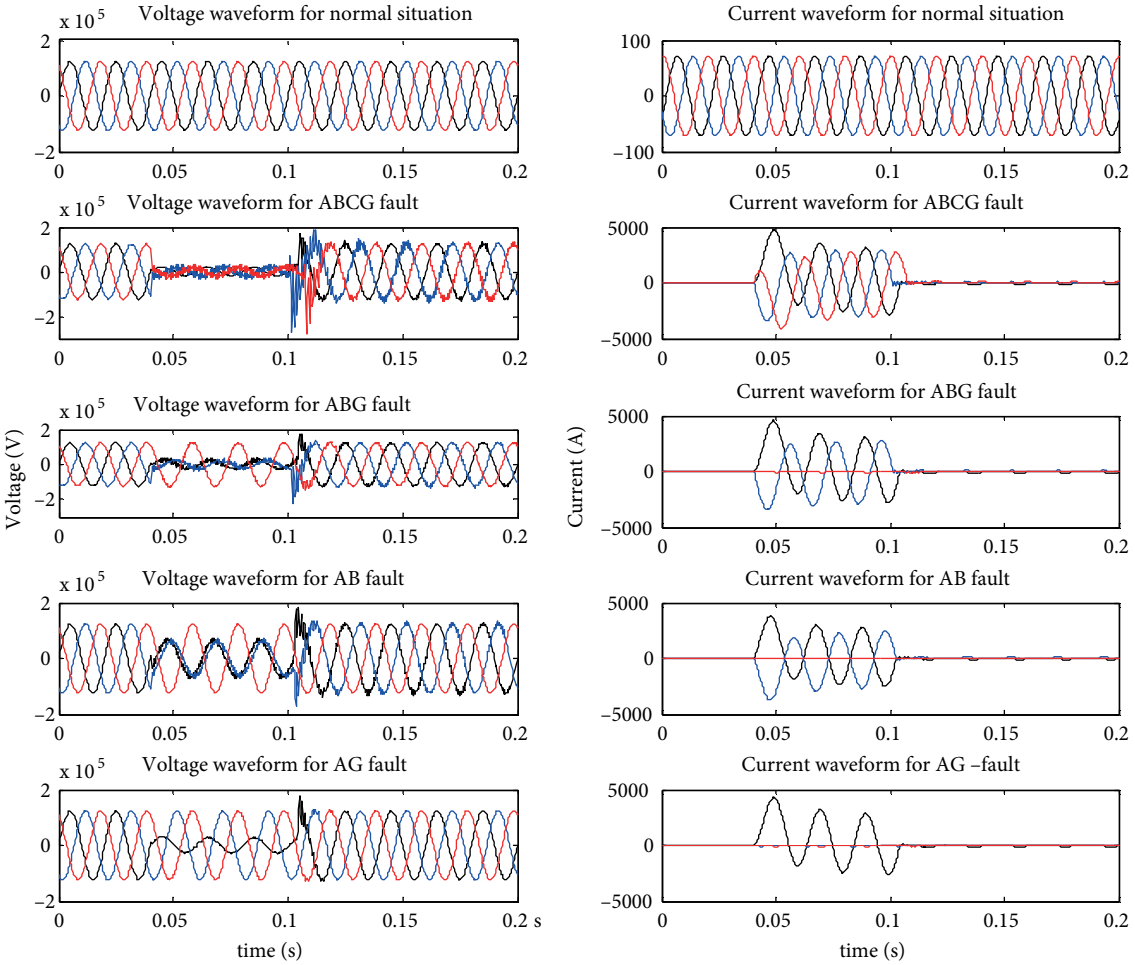

Figure 3. Three-phase current and voltage waveforms of the transmission line in nonfaulty and faulty conditions.

Table 2. Phase short-circuit types and the corresponding class labels with the number of signals for each class.

Phase short-circuit types	Class labels	Number of signals
Short circuit between A, B, C phases and ground	ABCG	440
Short circuit between A and B phases	AB	440
Short circuit between A, B phases and ground	ABG	440
Short circuit between A and C phases	AC	440
Short circuit between A, C phases and ground	ACG	440
Short circuit between A phase and ground	AG	440
Short circuit between B and C phases	BC	440
Short circuit between B, C phases and ground	BCG	440
Short circuit between B phase and ground	BG	440
Short circuit between C phase and ground	CG	440

Current and voltage waveforms measured from real power systems usually contain noise. Therefore, noise is added to the measured signals in order to simulate noise conditions occurring in real power systems. Four different noisy situations with a 20, 30, 40, and 50 dB signal-to-noise ratio (SNR) value are realized. Any SNR value of a signal is calculated as in Eq. (1):

$$SNR = 10 \log \left(\frac{P_s}{P_n} \right) (dB) , \tag{1}$$

where P_n is the power of the noise and P_s is the power (variance) of the signal. A peak noise magnitude of nearly 3.5% of the voltage signal is equivalent to a typical SNR value of 30 dB [25]. Current and voltage waveforms of a fault that occurred between phase A and the ground with a value of 20 dB SNR are shown in Figure 4.

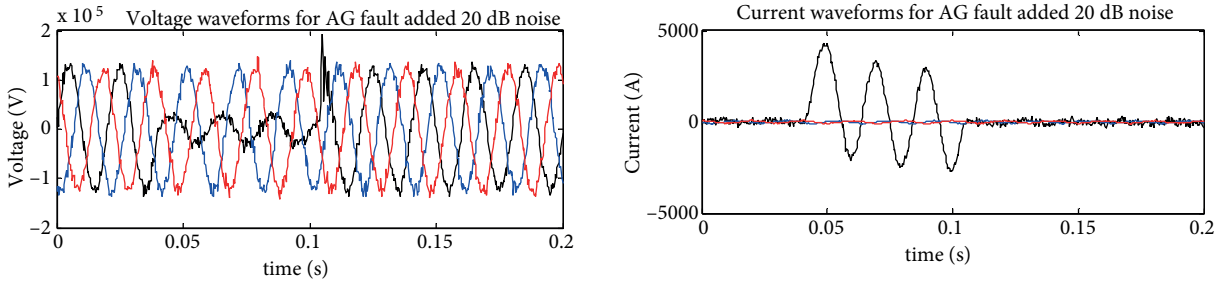

Figure 4. Current and voltage waveforms of fault that occurred between phase A and the ground with a value of 20 dB SNR.

4. Feature vector extraction

Feature extraction algorithms are the methods used to convert high-dimensional data to low-dimensional data with equivalent information content. Therefore, they are often used to reduce the size of data for decreasing the complexity of the classification or regression schemes [26]. Instantaneous active power components are thought to be more effective in the classification of short-circuit faults, because these signals have both current and voltage signal features. Therefore, feature extraction is performed by using instantaneous active power components. The specified simulation time is 0.2 s with 3.2 kHz of sampling frequency. Thus, there are 64 data

per period. The size of instantaneous current and voltage data for each phase in the voltage source side is 1 × 640. Instantaneous current and voltage data are normalized prior to feature extraction process using Eq. (2):

$$FC = \frac{FC}{\max\left(|FC\,[n]|\right)} \tag{2}$$

where n is the number of samples in the first simulation period before a fault occurrence. In Eq. (2), voltage and current signals are scaled per unit (pu) [27]. Both training and testing data are normalized according to the maximum current/voltage value of the related nonfaulty phase. The total active power is the sum of instantaneous active powers calculated for each phase in a three-phase system [28]. Gökmen [22] proposed a wavelet-based instantaneous active and reactive power calculation method. According to this method, it is possible to obtain DWT components of instantaneous active power by multiplying the DWT components of voltage and current.

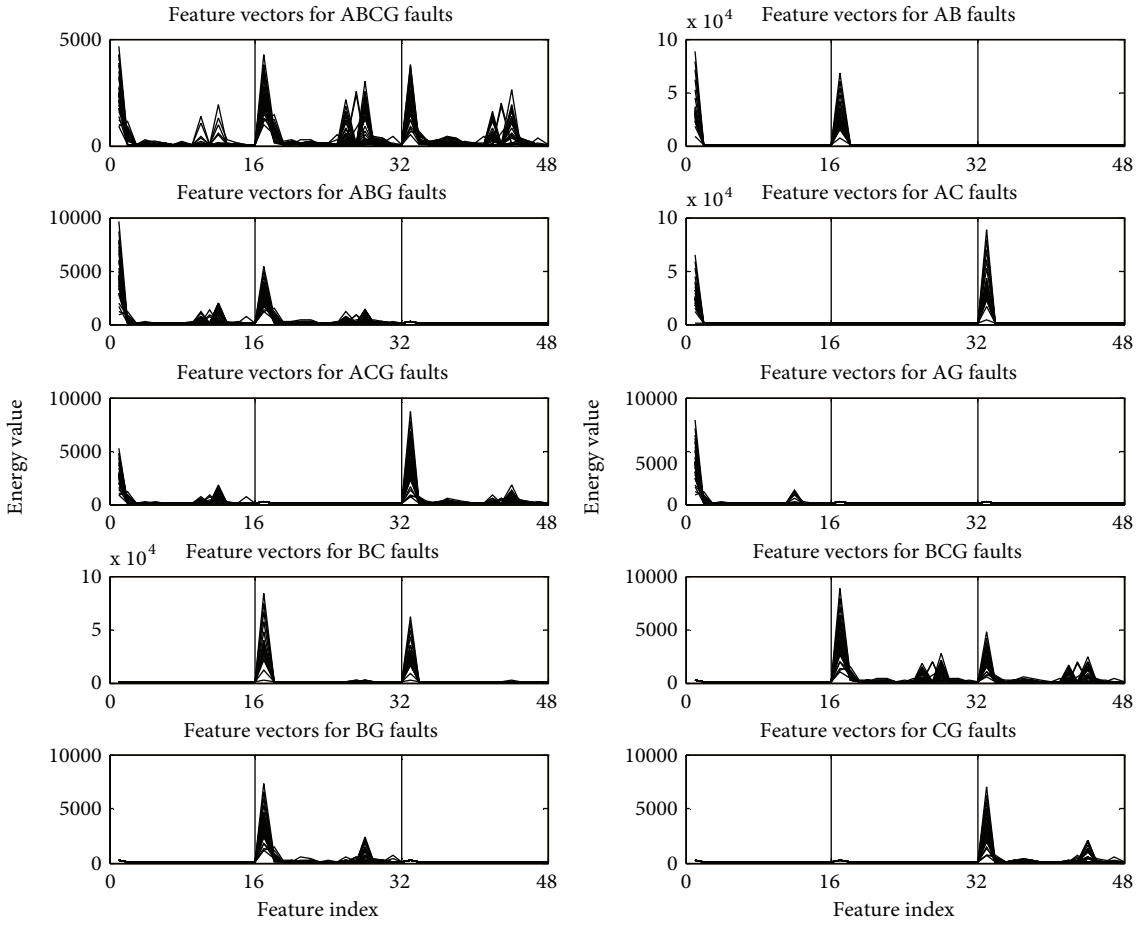

Figure 5. Various feature vectors based on the types of faults.

$$p_a = v_a.i_a = \left(\begin{array}{l} v_{AAAA4} + v_{DAAA4} + v_{ADAA4} + v_{DDAA4} + v_{AADA4} + v_{DADA4} + v_{ADDA4} + v_{DDDA4} + \\ v_{AAAD4} + v_{DAAD4} + v_{ADAD4} + v_{DDAD4} + v_{AADD4} + v_{DADD4} + v_{ADDD4} + v_{DDDD4} \end{array} \right).i_a \tag{3}$$

Four-level WPT is applied to normalized voltage data. Each voltage wavelet subband is then multiplied by the normalized current of the relevant phase, as seen in Eq. (3). In this way, 16 instantaneous active power components are obtained per phase. The size of each instantaneous active power component is 1 × 640. Thus, a total of 16 × 640 data are available for each phase. Since a three-phase system is investigated, there are 3 × 16 × 640 data in the overall experiment. An excessive amount of memory and time is required for processing 30,720 data. Signal energy is used for reducing data size and, in this way, the data do not lose their information content. The formulation of signal energy is given in Eq. (4).

$$E = \sum_{n=1}^{N} |v[n]|^2 \tag{4}$$

In Eq. (4), v is any signal, N is the number of samples included in the signal, and E is the energy of the signal. The energy of each instantaneous active power component is calculated for a phase. When they are arranged from the lower-frequency components to the higher ones, a feature vector with dimensions of 1 × 16 is constructed. The energy values of the other two phases are evaluated and concatenated in order to obtain a feature vector (1 × 48) for the entire three-phase system. The average duration of the feature vector extraction process is 0.1052 s per feature vector.

5. Classifiers and graphical user interface design

The SVM and ANN methods are most widely used in the studies of classification of the short circuits occurring in transmission lines. The CVA classifier was used in the diagnosis of the induction motor-bearing faults [29], phase-ground short circuit in low-voltage systems, and classification of four different faults exposed to two different loads [30]. In this paper, short circuits that occurred in high-voltage transmission line are classified. First, CVA is exploited as a classifier. The same training data are then treated with SVM and ANN for comparing the performances of the classifiers. The characteristics of CVA, SVM, and ANN classifiers, respectively, will be discussed in the following subsections.

The block diagram of the phase short-circuit fault classification is given in Figure 6.

5.1. Common vector approach

CVA is a classification method based on the separation of feature space into two subspaces, null space and range space. This method is broadly preferred in speech recognition [31,32], speaker identification [33], image classification [34], and motor fault diagnosis [29] problems. The main objective is to find a unique common vector that preserves the inherent characteristics of a pattern class. The CVA algorithm is performed separately for each class so that only within-class scatters of features are taken into account. The following steps are carried out to implement the CVA algorithm:

- The within-class covariance matrix (Φ) of a short circuit fault class is evaluated using the feature vectors of the corresponding class:

$$\Phi = \sum_{i=1}^{m} \left[(\mathbf{a}_i - \mathbf{a}_{ave}) (\mathbf{a}_i - \mathbf{a}_{ave})^T \right], \tag{5}$$

  where $\mathbf{a}_i$ is the ith feature vector in a fault class, m is the total number of feature vectors in the training set of each class, and $\mathbf{a}_{ave}$ is the average feature vector of the related class.

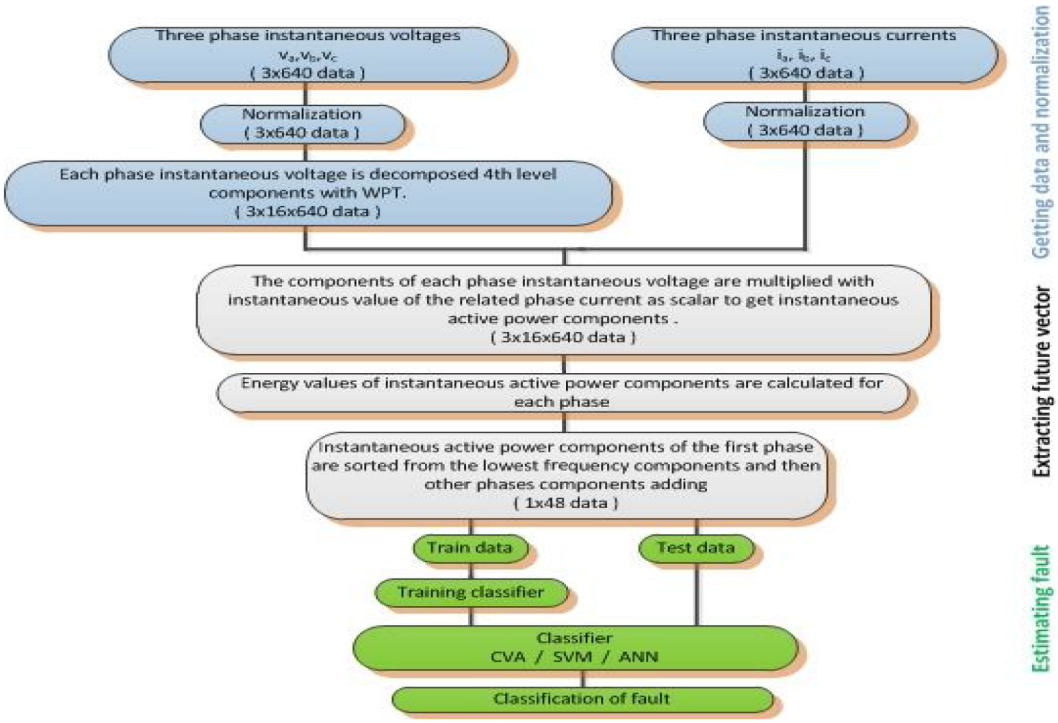

Figure 6. Block diagram of the phase short-circuit fault classification.

- The eigenvalues of Φ are semipositive and are sorted in descending order: $\lambda_1 \geq \lambda_2 \geq \ldots ... \geq \lambda_n$.
- The uppermost $(m-1)$ eigenvectors corresponding to the nonzero eigenvalues constitute an orthonormal basis vector set, spanning a subspace known as the difference subspace $\mathbf{B}$. The orthogonal complement $(\mathbf{B}^{\perp})$ is known as the indifference subspace spanned by the eigenvectors corresponding to the zero eigenvalues.
- Utilizing the linear combination of the eigenvectors corresponding to the zero eigenvalues, the common vector is calculated:

$$\begin{array}{l} \mathbf{a}_{com} = \langle \mathbf{a}_i, \mathbf{u}_m \rangle \mathbf{u}_m + \langle \mathbf{a}_i, \mathbf{u}_{m+1} \rangle \mathbf{u}_{m+1} + \ldots + \langle \mathbf{a}_i, \mathbf{u}_n \rangle \mathbf{u}_n \\ \forall i = 1, 2, \ldots, m \end{array} , \tag{6}$$

  where $\mathbf{a}_{com}$ is the common vector of the fault class and $\mathbf{u}_m, \mathbf{u}_{m+1}, ..., \mathbf{u}_n$ represents the orthonormal eigenvectors spanning the indifference subspace $(\mathbf{B}^{\perp})$ [29].
- In the test phase, an unknown feature vector, $\mathbf{a}_x$, is classified according to the following decision criterion:

$$class = \underset{1 \leq c \leq S}{argmin} \left\| \sum_{j=m}^{n} \left\{ \left[(\mathbf{a}_x - \mathbf{a}_{ave}^{c})^T \mathbf{u}_j^c \right] \mathbf{u}_j^c \right\} \right\|^2 , \tag{7}$$

  where $\mathbf{a}_{ave}^{c}$ is the average feature vector of the cth class, S is the number of the classes, and n indicates the total number of eigenvectors. This decision criterion assigns the test feature vector $(\mathbf{a}_x)$ to the cth class.

5.2. Support vector machine

SVM is a class of supervised learning algorithms. It was first introduced by Vapnik [35,36]. Pattern recognition problems, regression estimation problems, construction of intelligent machines, and forecasting are some of the SVM application areas.

SVM can be applicable to nonlinear and linear conditions. The separating margin between two classes is maximized by using SVM. The separating hyperplane $g(x)$ is given in Eq. (8) for linearly separable training data of two classes:

$$g\left(x\right) = w^T x + b = 0, \tag{8}$$

where w represents weight vectors, x is an input vector, b is bias, and $g(x)$ is output. Eq. (9) is solved for the maximum distance between two classes:

$$\min \frac{1}{2} w^T w, \tag{9}$$

and Eq. (10) is considered for minimizing the objective function in Eq. (9):

$$d_i \left(w^T x_i + b\right) \geq 1. \tag{10}$$

This problem can be solved by minimizing the Lagrange function. Eq. (11) is used for this minimization.

$$J\left(w, b, \alpha\right) = \frac{1}{2} w^T w - \sum_{i=1}^{p} \alpha_i \left[d_i \left(w^T x_i + b\right) - 1\right] \tag{11}$$

In Eq. (11), α is a nonzero Lagrange coefficient. Eqs. (9) and (10) have different forms when two classes are in a nonlinear case. The new objective function $\varnothing$ is given by:

$$\left(w, \xi\right) = \frac{1}{2} w^T w + C \sum_{i=1}^{p} \xi_i, \;\; \xi_i > 0, \tag{12}$$

$$d_i \left(w^T x_i + b\right) \geq 1 - \xi_i, \tag{13}$$

where C is the penalty factor and ξ is the slack variable. SVM maps the input vectors x into a high-dimensional space through some nonlinear mapping (φ function) in a nonlinear case [37,38]. Multiclass SVM could classify more than two classes. The one-against-one (OAO) and one-against-all (OAA) strategies are the most widely preferred methods [39–41]. In this paper, the Statistical Pattern Recognition Toolbox (STPRtool) for MATLAB is used for the SVM classifier [42]. The utilized versions of STPRtool and MATLAB are 2.11 and R2009b, respectively. The OAO strategy is preferred for the classification of short-circuit faults. The radial basis function (rbf) is chosen as the kernel function. The width parameter of rbf (γ) and penalty factor (C) are selected as 10,000 with trial-and-error learning.

5.3. Artificial neural network

An ANN is a mathematical model based on the structure of biological neuron cells. It obtains the knowledge given to it by processing. It is capable of implementing certain decision-making processes about new data. A multilayer neural network consists of an input layer, one or more hidden layers, and an output layer. Each layer contains numerous neurons. A neuron in each layer of the network is linked to nodes in the previous layer or to

other neurons [43]. The Neural Network Toolbox (nntool) for MATLAB is utilized in this paper. A three-layer feed-forward backpropagation network is applied for this study [1,9]. Although the number of neurons in the input and output layers depends on the number of input and output data, the number of neurons in the hidden layer is determined by the training performance of the network. Forty-eight neurons in the input layer, ten neurons in the hidden layer, and four neurons in the output layer are utilized in this paper. Sigmoid in the hidden layers and linear function in the output layers are applied as the activation functions. The network is trained by using the Levenberg–Marquardt backpropagation (TRAINLM) algorithm [44]. The adaption-learning function is chosen as gradient descent with momentum weight/bias (LEARNGDM), and the performance function is mean squared error (MSE). Four hundred data of a total of 4400 fault data are used for the training process of the ANN, and the remaining 4000 data are used for test process.

Since a normalization process is applied to the three-phase current and voltage data in the feature extraction stage, a data range of [–1, +1] is obtained. Although the measured output values are close to 1 in faulty conditions, they are close to 0 under normal conditions. A threshold value is identified to increase recognition accuracy. Classification performance of test data for various threshold values is given in Table 3. When the threshold values are chosen as 0.1, the highest recognition performance is obtained. If network output(s) are greater than 0.1, the case is accepted as faulty.

Table 3. Classification performance with respect to various threshold values for ANN.

	Threshold values						
	0.001	0.005	0.01	0.05	0.1	0.3	0.5
Noiseless	98.8%	98.525%	98.5%	97.975%	97.625%	96.85%	96.2%
20 dB	76.4%	90.2%	93.7%	99.35%	99.7%	99.6%	98.5%
30 dB	63.75%	83%	90.35%	99.125%	99.15%	99.05%	98.675%
40 dB	36.375%	40.025%	42%	90.075%	99.55%	98.775%	97.725%
50 dB	69.05%	82.175%	88.075%	97.375%	98.8%	98.725%	97.45%
Average	68.875%	78.785%	82.525%	96.78%	98.965%	98.6%	97.71%

SVM has certain important advantages compared to ANNs. The error function has many local minima, and hence a learning process may fail. Furthermore, a learning algorithm cannot control the complexity of the architecture of ANN; therefore, this architecture determines the generalization abilities [36,45–51].

5.4. GUI design

A graphical user interface (GUI) is designed by using the MATLAB/GUI application and it is shown in Figure 7. This interface provides several facilities, such that a user can classify short-circuit faults with different classifiers, set the required parameters, and generate various short-circuit faults on the transmission line.

Fault type, source frequency, fault distance, fault inception angle, and fault duration can be easily adjusted with this developed interface. In addition, different amplitudes of fault types can be specified. Noises with various SNR values can be added to current and voltage signals. Current, voltage, and feature vector waveforms of the desired phase(s) can be easily sketched. Furthermore, the type of classifier preferred in fault classification is readily determined by using this interface. The window where the plots are sketched can be shifted, and waveforms can be expanded or narrowed with a magnifying glass. It is possible to read a value at any desired point in a plot.

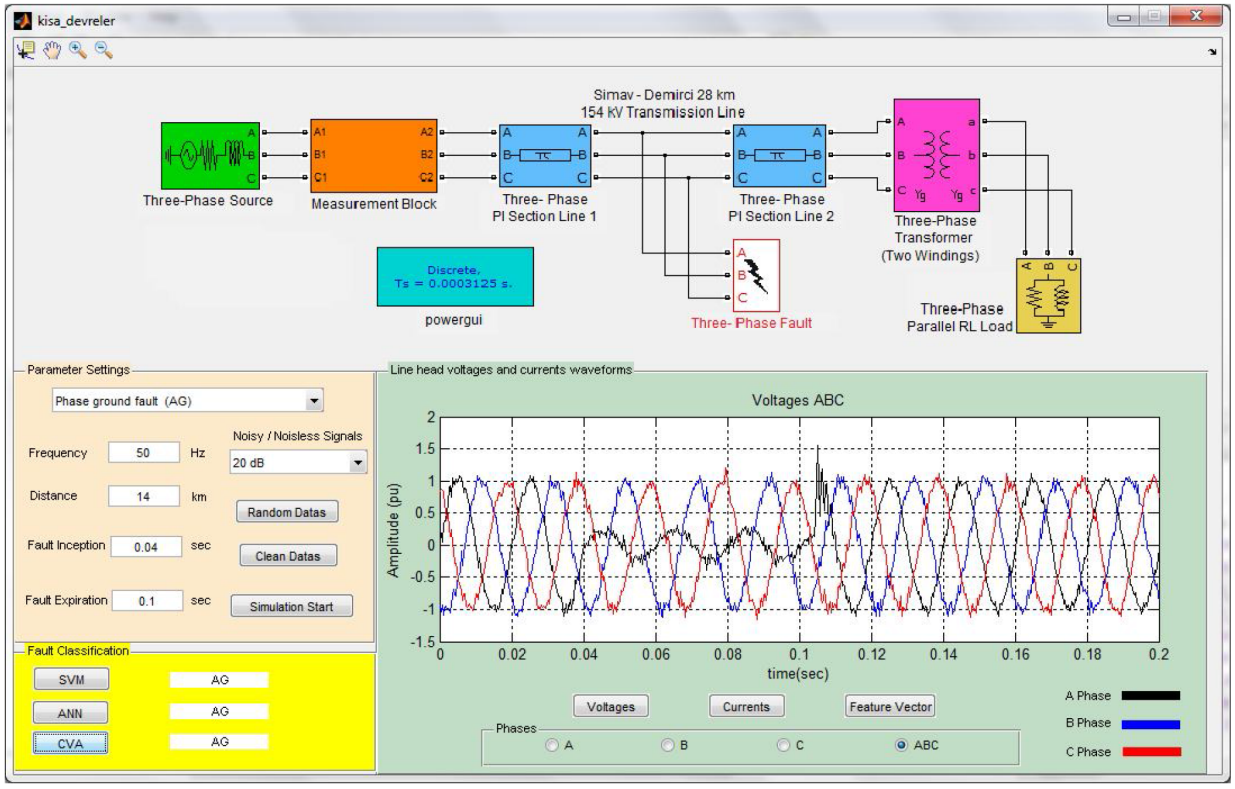

Figure 7. GUI of phase short-circuit classifier.

6. Results and discussion

In this paper, the real parameters of a 28 km, 154 kV transmission line between Simav and Demirci in Turkey's electricity transmission network are simulated in MATLAB/Simulink. The system frequency is controlled in a range of 49.8–50.2 Hz (approximately 50 Hz), according to the regulations [52]. The fault inception angle is between 0° and 360° . Additionally, the fault distance is in the interval of 0.01 and 27.99 km from the beginning of the line, and the fault exposure duration is between 0.01 and 0.2 s. In total, ten different short-circuit conditions are classified: phase-ground, phase-phase, two phase-ground, and three phase-ground. Ten different source frequencies, 10 different fault inception angles, 10 different fault exposure durations, and 10 different fault distances are generated for each fault. Therefore, the training process is achieved with a total of 400 data. One hundred different source frequencies, 100 different fault inception angles, 100 different fault exposure durations, and 100 different fault distances are also produced for each fault. In total, 4000 data are used in the test process. All noiseless testing data are correctly classified by using the CVA classifier. Classification performances of noiseless faults, using the proposed feature extraction scheme with the SVM and ANN methods, are given in Tables 4 and 5, respectively.

Classification performances of the same training and test data are examined when they are exposed to noise with SNR values of 20, 30, 40, and 50 dB. Table 6 presents the accuracies for the classification of faults using CVA, SVM, and ANN for noiseless and noisy cases. It is clearly seen that CVA gives the best classification results with the 99.965% average performance.

Table 4. Classification performance of noiseless faults using SVM.

Fault	ABCG	AB	ABG	AC	ACG	AG	BC	BCG	BG	CG	Accuracy (%)
ABCG	399	0	0	0	0	0	0	1	0	0	99.75%
AB	0	400	0	0	0	0	0	0	0	0	100%
ABG	1	0	399	0	0	0	0	0	0	0	99.75%
AC	0	0	0	394	6	0	0	0	0	0	98.5%
ACG	0	0	0	0	399	0	0	0	0	1	99.75%
AG	0	0	0	0	0	400	0	0	0	0	100%
BC	0	0	0	0	0	0	399	1	0	0	99.75%
BCG	0	0	0	0	0	0	1	399	0	0	99.75%
BG	0	0	0	0	0	0	0	0	400	0	100%
CG	0	0	0	0	0	0	0	0	0	400	100%
Overall classification accuracy						99.725%					

Table 5. Classification performance of noiseless faults using ANN.

Fault	ABCG	AB	ABG	AC	ACG	AG	BC	BCG	BG	CG	Accuracy (%)
ABCG	367	0	0	0	0	0	0	16	0	0	91.75%
AB	0	400	0	0	0	0	0	0	0	0	100%
ABG	0	37	363	0	0	0	0	0	0	0	90.75%
AC	0	0	0	400	0	0	0	0	0	0	100%
ACG	0	0	0	10	389	0	0	0	0	1	97.25%
AG	0	0	0	0	0	396	0	0	0	0	99%
BC	0	0	0	0	0	0	400	0	0	0	100%
BCG	4	0	0	0	0	0	2	394	0	0	98.5%
BG	0	0	0	0	0	0	0	0	398	0	99.5%
CG	0	0	0	0	2	0	0	0	0	398	99.5%
Overall classification accuracy						97.625%					

Table 6. Comparison of classification performances of faults using CVA, SVM, and ANN methods for noiseless and noisy circumstances.

	Noiseless	20 dB	30 dB	40 dB	50 dB	Average
CVA	100%	99.875%	99.975%	100%	99.975%	99.965%
SVM	99.725%	99.55%	99.75%	99.8%	99.75%	99.715%
ANN	97.625%	99.7%	99.15%	99.55%	98.8%	98.965%

Training and testing durations of CVA, SVM, and ANN methods for both noiseless and noisy data are measured and given in Table 7. It can be easily deduced that SVM is the fastest classifier for the test stage, whereas CVA is the fastest classifier for the training stage. A notebook used to measure these durations has a microprocessor of Intel Core i7-740QM 1.73 GHZ and a memory of 4 GB.

Table 7. Training and testing durations of CVA, SVM, and ANN methods for noiseless and noisy data cases.

		Noiseless	20 dB	30 dB	40 dB	50 dB
CVA	Train (s)	0.035551	0.036630	0.036098	0.037542	0.038225
	Test (s)	0.002941	0.002924	0.002947	0.002959	0.002960
SVM	Train (s)	0.038229	0.043289	0.040668	0.040350	0.039428
	Test (s)	0.000789	0.000829	0.000797	0.000743	0.000741
ANN	Train (s)	4	3	4	5	4
	Test (s)	0.006705	0.006668	0.006878	0.006809	0.006799

7. Conclusion

In this paper, a new feature extraction scheme is based on the energies of instantaneous active power components for the classification of phase short-circuit faults that occurred in high-voltage transmission lines. An electricity transmission network is simulated by using the real parameters of a 28 km, 154 kV transmission line between Simav and Demirci. A normalization process was first applied to instantaneous current and voltage data measured from the voltage source side of the transmission line. Instantaneous active power components were obtained by multiplying normalized instantaneous current and WPT-decomposed instantaneous voltage data. Feature vectors were constructed using energies of instantaneous active power components. These feature vectors were then classified by CVA. This situation is the first implementation of CVA on the classification of short-circuit faults occurring in high-voltage energy transmission lines. Furthermore, the same feature vectors were applied to both SVM and ANN for a comparison with the CVA method in terms of recognition accuracy and testing duration issues.

Noises with various SNR values (20, 30, 40, and 50 dB) were added to the raw voltage and current data. Therefore, the simulated signals exactly resembled real faulty signals. The best results were attained with the CVA method. The CVA classifier is simple, fast, and robust for both noise conditions and various fault parameters.

Moreover, a graphical user interface was designed using MATLAB. Short circuit faults can be quite easily classified with this interface. The fault parameters can be readily adjusted and their corresponding effects on short-circuit faults can be explicitly traced by means of this interface.

Acknowledgment

This paper was supported by the Scientific Research Projects Coordinating Office of Marmara University (Project No. FEN-C-DRP-161111-0300).

References

[1] Geethanjali M, Priya KS. Combined wavelet transforms and neural network (WNN) based fault detection and classification in transmission lines. In: IEEE 2009 Conference on Control, Automation, Communication and Energy Conservation; 4–6 June 2009; Perundurai, India. New York, NY, USA: IEEE. pp. 1-7.

[2] Ekici S, Yildirim S, Poyraz M. A transmission line fault locator based on Elman recurrent networks. Appl Soft Comput 2009; 9: 341-347.

[3] Bhowmik PS, Purkait P, Bhattacharya K. A novel wavelet transform aided neural network based transmission line fault analysis method. Int J Elec Power 2009; 31: 213-219.

[4] Erişti H, Demir Y. A new algorithm for automatic classification of power quality events based on wavelet transform and SVM. Expert Syst Appl 2010; 37: 4094-4102.

[5] Chanda D, Kishore NK, Sinha AK. Application of wavelet multiresolution analysis for identification and classification of faults on transmission lines. Electr Pow Syst Res 2005; 73: 323-333.

[6] Reddy MJ, Mohanta DK. A wavelet-fuzzy combined approach for classification and location of transmission line faults. Int J Elec Power 2007; 29: 669-678.

[7] El Safty S, El-Zonkoly A. Applying wavelet entropy principle in fault classification. Int J Elec Power 2009; 31: 604-607.

[8] Upendar J, Gupta CP, Singh GK, Ramakrishna G. PSO and ANN-based fault classification for protective relaying. IET Gen Trans Dis 2010; 4: 1197-1212.

[9] Abdollahi A, Seyedtabaii S. Comparison of Fourier & wavelet transform methods for transmission line fault classification. In: IEEE 2010 International Conference on Power Engineering and Optimization; 23–24 June 2010; Shah Alam, Malaysia. New York, NY, USA: IEEE. pp. 579-584.

[10] Samantaray SR. A systematic fuzzy rule based approach for fault classification in transmission lines. Appl Soft Comput 2013; 13: 928-938.

[11] Joorabian M, Taleghani Asl SMA, Aggarwal RK. Accurate fault locator for EHV transmission lines based on radial basis function neural networks. Electr Pow Syst Res 2004; 71: 195-202.

[12] Jamehbozorg A, Shahrtash SM. A decision-tree-based method for fault classification in single-circuit transmission lines. IEEE T Power Deliver 2010; 25: 2190-2196.

[13] He Z, Fu L, Lin S, Bo Z. Fault detection and classification in EHV transmission line based on wavelet singular entropy. IEEE T Power Deliver 2010; 25: 2156-2163.

[14] Ekici S. Support vector machines for classification and locating faults on transmission lines. Appl Soft Comput 2012; 12: 1650-1658.

[15] Çöteli R. A combined protective scheme for fault classification and identification of faulty section in series compensated transmission lines. Turk J Electr Eng Co 2013; 21: 1842-1856.

[16] Misiti M, Misiti Y, Oppenheim G, Poggi JM. Wavelet Toolbox for Use with MATLAB. User's Guide Version 2. Natick, MA, USA: The MathWorks, 2002.

[17] Özgönenel O, Önbilgin G, Kocaman Ç. Transformer protection using the wavelet transform. Turk J Electr Eng Co 2005; 13: 119-135.

[18] Zang H, Zhao Y. Intelligent identification system of power quality disturbance. In: IEEE 2009 Global Congress on Intelligent Systems; 19–21 May 2009; Xiamen, China. New York, NY, USA: IEEE. pp. 258-261.

[19] Arikan Ç, Özdemir M. Wavelet approach and skewness-kurtosis coefficients on the detection of some power quality disturbances in power systems. In: TMMOB 2012 Elektrik-Elektronik ve Bilgisayar Mühendisliği Sempozyumu; 29 November–1 December 2012; Bursa, Turkey. Bursa, Turkey: TMMOB. pp. 128-132 (in Turkish).

[20] Patel M, Patel RN. Fault detection and classification on a transmission line using wavelet multi resolution analysis and neural network. Int J Comput Appl 2012; 47: 27-33.

[21] El-Zonkoly AM, Desouki H. Wavelet entropy based algorithm for fault detection and classification in FACTS compensated transmission line. Int J Elec Power 2011; 33: 1368-1374.

[22] Gökmen G. Wavelet based instantaneous reactive power calculation method and a power system application sample. Int Rev Mod Sim 2011; 4: 745-752.

[23] Gokmen G. Wavelet based reference current calculation method for active compensation systems. Elektron Elektrotech 2011; 2: 61-66.

[24] Eren Z, Aktaş K, İyiiş B. Türkiye Ulusal Elektrik Ağındaki Havai Hatların, Trafoların ve Generatörlerin Elektriki Karakteristikleri. Ankara, Turkey: TEK, 2005 (in Turkish).

[25] Uyar M, Yildirim S, Gencoglu MT. An effective wavelet-based feature extraction method for classification of power quality disturbance signals. Electr Pow Syst Res 2008; 78: 1747-1755.

[26] Yusuff AA, Fei C, Jimoh AA, Munda JL. Fault location in a series compensated transmission line based on wavelet packet decomposition and support vector regression. Electr Pow Syst Res 2011; 81: 1258-1265.

[27] Uyar M. Identification of power quality disturbance types by using intelligent pattern recognition approach. PhD, Fırat University, Elazığ, Turkey, 2008 (in Turkish).

[28] Peng FZ, Lai JS. Generalized instantaneous reactive power theory for three-phase power systems. IEEE T Instrum Meas 1996; 45: 293-297.

[29] Gülmezoğlu MB, Ergin S. An approach for bearing fault detection in electrical motors. Eur T Electr Power 2007; 17: 628-641.

[30] Gerek ÖN, Ece DG, Barkana A. Covariance analysis of voltage waveform signature for power-quality event classification. IEEE T Power Deliver 2006; 21: 2022-2031.

[31] Gulmezoglu MB, Dzhafarov V, Keskin M, Barkana A. A novel approach to isolated word recognition. IEEE T Speech Audi P 1999; 7: 620-628.

[32] Gulmezoglu MB, Dzhafarov V, Barkana A. The common vector approach and its relation to principal component analysis. IEEE T Speech Audi P 2001; 9: 655-662.

[33] Gülmezoğlu MB, Barkana A. Text-dependent speaker recognition by using Gram–Schmidt orthogonalization method. In: IASTED 1998 International Conference on Signal Processing and Communications; 1–4 February 1998; Canary Islands, Spain. Calgary, Canada: IASTED. pp. 438-440.

[34] Cevikalp H, Neamtu M, Wilkes M, Barkana A. Discriminative common vectors for face recognition. IEEE T Pattern Anal 2005; 27: 4-13.

[35] Vapnik VN. An overview of statistical learning theory. IEEE T Neural Network 1999; 10: 988-999.

[36] Yu X, Wang K. Digital system for detection and classification of power quality disturbance. In: IEEE 2009 Power and Energy Engineering Conference; 27–31 March 2009; Wuhan, China. New York, NY, USA: IEEE. pp. 1-4.

[37] Chua KS. Efficient computations for large least square support vector machine classifiers. Pattern Recogn Lett 2003; 24: 75-80.

[38] Salat R, Osowski S. Accurate fault location in the power transmission line using support vector machine approach. IEEE T Power Syst 2004; 19: 979-986.

[39] Hsu CW, Lin CJ. A comparison of methods for multiclass support vector machines. IEEE T Neural Networ 2002; 13: 415-425.

[40] Kocaman C, Usta H, Ozdemir M, Eminoglu I. Classification of two common power quality disturbances using wavelet-based SVM. In: IEEE 2010 Mediterranean Electrotechnical Conference; 26–28 April 2010; Valletta, Malta. New York, NY, USA: IEEE. pp. 587-591.

[41] Yıldırım S. The using of support vector machines in fault diagnosis. MSc, Fırat University, Elazığ, Turkey, 2006 (in Turkish).

[42] Franc V, Hlavac, V. Statistical Pattern Recognition Toolbox for MATLAB. User's Guide. Prague, Czech Republic: Czech Technical University, 2010.

[43] Haykin, S. Neural Networks: A Comprehensive Foundation. 2nd ed. New Delhi, India: Prentice Hall, 1999.

[44] Demuth H, Beale M, Hagan M. Neural Network Toolbox 6. User's Guide. Natick, MA, USA: The MathWorks, 2009.

[45] Hsieh JG. Lecture Notes on Support Vector Machines. Taipei, Taiwan: National Sun Yat-Sen University, 2003.

[46] Gunn SR. Support Vector Machines for Classification and Regression. Southampton, UK: Southampton University, 1998.

[47] Burges CJC. A tutorial on support vector machines for pattern recognition. Data Min Knowl Disc 1998; 2: 121-167.

[48] Liu X, Fu H. A hybrid algorithm for text classification problem. Prz Electrotechniczn 2012; 1b: 8-11.

[49] Ekici S. Classification of power system disturbances using support vector machines. Expert Syst Appl 2009; 36: 9859-9868.

[50] Patterson DW. Artificial Neural Networks: Theory and Applications. London, UK: Prentice Hall, 1996.

[51] Cichocki A, Unbehauen R. Neural Networks for Optimization and Signal processing. New York, NY, USA: Wiley, 1993.

[52] EPDK. Elektrik Iletim Sistemi Arz Güvenilirliği ve Kalitesi Yönetmeliği. Ankara, Turkey: Enerji PiyasasıDüzenleme Kurumu, 2013 (in Turkish).

Appendix. Parameters of equipment used in the model.

Equipment	Parameters	
Generator	Voltage: 154 kV	Internal connection: Yg
	3-phase short-circuit level at base voltage (VA): 667 MVA	
	X/R:7	
Transmission line	Line voltage: 154 kV	Line length: 28 km
	$R_+ = 0.135714\ \Omega$/km	$R_0 = 0.417857\ \Omega$/km
	$L_+ = 0.001375$ H/km	$L_0 = 0.003853$ H/km
	$C_+ =$ 8.344266e-9 F/km	$C_0 =$ 6.513984e-9 F/km
Transformer (Yg/Yg)	Voltage: 154/34.5 kV	Power: 16 MVA
	R1 = 4.633 Ω	L1 = 0.2666 H
	R2 = 0.23252 Ω	L2 = 0.01338 H
	Magnetization resistance	Rm = 1285004.1525 Ω
	Magnetization inductance	Lm = 528.9090 H
Load (Yg)	Voltage: 34.5 kV	Active power P = 12.8 MW
	Inductive reactive power	QL= 9.6 MVAR